



Published in final edited form as:

*Environ Microbiol Rep.* 2015 April ; 7(2): 330–340. doi:10.1111/1758-2229.12252.

## The exopolysaccharide Psl–eDNA interaction enables the formation of a biofilm skeleton in *Pseudomonas aeruginosa*

Shiwei Wang<sup>1</sup>, Xi Liu<sup>1,2</sup>, Hongsheng Liu<sup>3</sup>, Li Zhang<sup>3</sup>, Yuan Guo<sup>4</sup>, Shan Yu<sup>1,2</sup>, Daniel J. Wozniak<sup>5</sup>, and Luyan Z. Ma<sup>1,\*</sup>

<sup>1</sup>State Key Laboratory of Microbial Resources, Institute of Microbiology, Chinese Academy of Sciences, Beijing 100101, China

<sup>2</sup>University of the Chinese Academy of Sciences, Beijing 100049, China

<sup>3</sup>School of Life Science, Liaoning University, Shenyang 110036, China

<sup>4</sup>Center for Applied Geosciences, Eberhard Karls University Tuebingen, Tuebingen 72074, Germany

<sup>5</sup>Department of Microbial Infection and Immunity, Department of Microbiology, Center for Microbial Interface Biology, The Ohio State University, Columbus, OH 43210, USA

### Summary

A hallmark of bacterial biofilms is a self-produced extracellular matrix of exopolysaccharide, extracellular DNA (eDNA) and proteins that hold bacterial cells together in the community. However, interactions among matrix components and how the interactions contribute to the formation of matrix remain unclear. Here, we show the physical interaction between exopolysaccharide Psl and eDNA, the two key biofilm matrix components of the opportunistic pathogen *Pseudomonas aeruginosa*. The interaction allows the two components to combine to form a web of eDNA–Psl fibres, which resembles a biofilm skeleton in the centre of pellicles to give bacteria structural support and capability against agents targeted on one matrix component. The web of eDNA–Psl fibres was also found in flow-cell biofilms at microcolonies initiation stage. The colocalization of eDNA or Psl fibres with bacterial cell membrane stain suggests that fibre-like eDNA is likely derived from the lysis of dead bacteria in biofilms. Psl can interact with DNA from diverse sources, suggesting that *P. aeruginosa* has the ability to use DNA of other organisms (such as human neutrophils and other bacterial species) to form its own communities, which might increase the survival of *P. aeruginosa* in multispecies biofilms or within a human host.

### Introduction

The complex multicellular communities of microorganisms known as biofilms are of high significance to industrial, environmental and clinical settings. Biofilms, for example, are a

\*correspondence. luyanma27@im.ac.cn; Tel.86 10 64806101; Fax 86 10 64807437.

Supporting information: Additional Supporting Information may be found in the online version of this article at the publisher's website:

source of persistent infections (Costerton *et al.*, 1999). The biofilm matrix is a poorly defined mixture of extracellular DNA (eDNA), exopolysaccharides and proteins that enmesh microbial cells together into a community and provide protection for resident cells in the biofilm. To date, the interactions among the components of the biofilm matrix, especially between two critical components, eDNA and exopolysaccharide, remain unclear.

Extracellular DNA is an important and abundant matrix component of many single- and multispecies cultured biofilms (Whitchurch *et al.*, 2002; Flemming and Wingender, 2010). Extracellular DNA strengthens biofilms, confers antibiotic resistance, and acts as a nutrient source during starvation and a gene pool for the horizontal gene transfer (Molin and Tolker-Nielsen, 2003; Dominiak *et al.*, 2011; Chiang *et al.*, 2013). Extracellular DNA can also facilitate twitching motility-mediated biofilm expansion (Gloag *et al.*, 2013). That eDNA functions as a matrix component was first reported in *Pseudomonas aeruginosa*, an important opportunistic pathogen and a paradigm organism for biofilm research (Whitchurch *et al.*, 2002). DNase I can disrupt ‘young’ but not established, ‘aged’ biofilms of *P. aeruginosa* (Whitchurch *et al.*, 2002; Parks *et al.*, 2009), suggesting the complexity and dynamic of biofilm matrix. As a matrix component, eDNA is mostly found in microbial communities rather than in the tissues of animals and plants.

Unlike eDNA, exopolysaccharide is a common matrix component in plant and animal. It is also a critical biofilm matrix component of many Gram-positive and Gram-negative bacteria (Ma *et al.*, 2009; Kolodkin-Gal *et al.*, 2012; Xiao *et al.*, 2012). Despite highly aggressive antimicrobial therapy, *P. aeruginosa* (a Gram-negative bacterium) causes life-threatening, persistent infections in cystic fibrosis (CF) patients. Persistence is due to the ability of these bacteria to form biofilms (Singh *et al.*, 2000). Thus, many studies have focused on biofilm formation of *P. aeruginosa*. Exopolysaccharide Psl is a key scaffolding component in *P. aeruginosa* that promotes bacterial cell–cell and cell–surface interactions by acting as ‘molecular glue’; Psl forms a fibre-like matrix to maintain the biomass of flow-cell biofilms as well as floating biofilms known as pellicles at the air–liquid interface of standing cultures (Ma *et al.*, 2009; Wang *et al.*, 2013). Psl can also function as a signal to stimulate biofilm formation by *P. aeruginosa* (Irie *et al.*, 2012). Researchers have proposed that the formation of Psl fibres or tracks is a result of Psl release from the bacterial cell surface during bacterial migration mediated by type IV pili (Wang *et al.*, 2013). Zhao and colleagues (2013) also showed that *P. aeruginosa* could deposit Psl trails during migration on a surface and that such trails guided subsequent bacterial exploration, leading to the formation of microcolonies (Zhao *et al.*, 2013).

In this study, we demonstrate the existence of the physical interaction between eDNA and Psl, which enables the formation of an eDNA–Psl–membrane combined fibres web in the centre of biofilms, resembling a skeleton of biofilms. Psl can interact not only with DNA of *P. aeruginosa*, but also the genomic DNA from human neutrophils and Gram-positive bacterium *Staphylococcus aureus*, implying that *P. aeruginosa* has the ability to use DNA of other organisms to form its own communities.

## Results and discussion

### A skeleton-like web of eDNA–Psl fibres located in the centre of air–liquid interface biofilms (pellicles) of *P. aeruginosa* PAO1

We previously showed that the exopolysaccharide Psl can form a fibre-like matrix in pellicles and flow-cell biofilms of *P. aeruginosa* (Wang *et al.*, 2013). While detecting DNA in *P. aeruginosa* pellicles with SYTO9, a green fluorescent DNA dye that stains genomic DNA within bacteria (concentrated fluorescent dot) as well as eDNA (diffused fluorescence or fibre-like structure) in biofilms, we found that eDNA can form a fibre-like structure similar to the Psl matrix. The DNA fibre-like structure was frequently observed in an established pellicle that was several micrometres thick (Fig. 1A and B). Analysis of 45 image stacks indicated that the frequency of DNA fibres observed in 2 day old pellicles was over 90%. Like the Psl fibre matrix in pellicles (Wang *et al.*, 2013), the DNA fibre web has a radial pattern and is located in the middle of pellicles (Fig. 1B). By using the DNA dye SYTO9 along with the Psl-staining *Hippeastrum hybrid* lectin from *amarillis* (HHA), we found that most of the fibre-like DNA was colocalized with Psl fibres in *P. aeruginosa* pellicles (Fig. 1C; Fig. S1). The analysis of five image stacks by three different methods showed that the DNA–Psl colocalization coefficients were all above 0.5 (Fig. 2). The visible DNA–Psl colocalization was mostly associated with a fibre-like/rope-like matrix structure (Fig. 1C and E; Fig. S1). Such eDNA–Psl fibres were mostly found in the middle to the air face of pellicles (Fig. 2; Fig. S1). The DNA–Psl fibre structure resembled a ‘skeleton’ of biofilms or backbones that was located at the centre of pellicles and that was surrounded by bacteria (Fig. 1A–F). The eDNA–Psl fibres that had strong fluorescent signals (indicated by a big arrow in Fig. 1F) or had weak fluorescent signals (indicated by a small arrow in Fig. 1F) were both found in a pellicle.

To further confirm that the DNA fibres were eDNA, we used propidium iodide (PI), a red fluorescent dye that is not permeable to cell membranes. PI is often used for staining eDNA in biofilms and it can also stain genomic DNA within bacteria that had compromised cell membranes. Thus bacterial cells stained by PI is considered to be dead or dying. The results of PI and SYTO9 double stainings showed that SYTO9-stained DNA fibres in pellicles were overlapped with eDNA fibres stained by PI (Fig. 3A). In contrast, little overlapping was found between SYTO9-stained genomic DNA within live bacteria and PI-stained genomic DNA in dead bacteria (Fig. 3A). This data further confirmed that DNA fibres in pellicles were eDNA. In addition, PI and Psl double stainings also indicated the colocalization of eDNA fibres and Psl (Fig. 3B).

### The eDNA–Psl fibres are also present in flow-cell biofilms

Double staining with SYTO9/HHA-TRITC (Fig. 4A) or PI/HHA-FITC (Fig. 4B) indicated that eDNA colocalized with Psl and formed fibre-like structures in flow-cell biofilms at microcolonies initiation stage. Most of the eDNA–Psl combined fibres were either surrounding multiple bacterial cell aggregates or in areas with a few bacteria (Fig. 4). The distribution pattern was similar to that of Psl fibre matrices in flow-cell biofilms reported previously (Wang *et al.*, 2013). Some eDNA–Psl fibres (indicated by the white arrows in Fig. 4) were also visualized in differential interference contrast (DIC) images. Many dead

cells that were stained by PI and had a localized staining pattern (indicated by the black arrow in Fig. 4B) were often associated with eDNA–Psl fibres. The web of eDNA–Psl fibres in flow-cell biofilms did not appear identical to the web of eDNA–Psl fibres in pellicles. The differences in the pattern of eDNA–Psl fibres in pellicles versus flow-cell biofilms were most likely due to differences in growth conditions and flow stress. The flow-cell biofilms were attached to a solid glass surface and grew with continuously flowing media, while the pellicles were floating on liquid media with limited flow. Taken together, our data suggested that the Psl–eDNA association and the formation of eDNA–Psl fibres were not specific to air–liquid interface biofilms but occurred in both types of biofilms.

### **eDNA fibres were likely derived from dead bacteria in biofilms**

While a living bacterial cell is doubly-stained by SYTO9 and FM4-64, the genomic DNA appears usually as a concentrate fluorescent dot within bacterial cell membrane. The DNA fibres visualized in pellicles were overlapped with bacterial membrane stained by FM4-64 (Fig. 1D) and DNA stained by PI (Fig. 3), which suggested that eDNA fibres were likely derived from dead or dying bacteria (membrane-compromised bacteria). In support of this suggestion, a track of bacterial cell membrane staining was observed in a flow-cell biofilm that appeared following a bacterial cell and was colocalized with Psl staining (Fig. 4C). This membrane track was also clearly visible in the DIC image (indicated by big white arrows in Fig. 4C), which was similar to the eDNA–Psl fibres depicted in Fig. 4A and B. The membrane of a live bacterium would not be likely peeled off to leave a membrane track; thus, these results suggested that eDNA fibres were likely derived from dead bacteria in biofilms, and flow stress might peel off the membrane of membrane-compromised bacteria and stretch out their chromosome DNA, leading to the formation of eDNA–Psl-membrane fibres.

Previous reports have not found detectable eDNA associated with Psl trails/tracks from living bacteria (Wang *et al.*, 2013; Zhao *et al.*, 2013). Psl released from a living bacterium may be associated with limited eDNA ( $\approx 2.5 \times 10^{-8}$   $\mu\text{g}$  per bacterial cell) (Allesen-Holm *et al.*, 2006), which may be under the fluorescence-detecting level. The formation of Psl–eDNA fibres with strong fluorescent signals (Fig. 1F, the stronger fluorescent signal indicates that the fibre has more Psl and DNA material) is likely a result of multiple events (such as lysis of multiple bacteria). Initially, the eDNA or Psl–eDNA tracks may have a weak fluorescent signal (such as the one indicated by the small arrow in Fig. 1F). However, bacteria attached to eDNA or Psl–eDNA fibres (or tracks) may die, and their DNA and Psl may merge with the original fibre and thereby increase their volume.

### **Psl interacts with DNA from diverse sources**

The association of eDNA and Psl in biofilms suggested that there may be physical interaction between the two components. To determine whether there is physical interaction between the two main biofilm matrix components, Psl and eDNA, we used a modified competitive binding assay. Psl can be coated on microtiter plates and detected by ELISA with anti-Psl serum (Byrd *et al.*, 2010); thus, the blocking of Psl coated on wells of ELISA plates by DNA represents a form of competitive binding assay that tests the interaction between Psl and DNA. To perform the assay, we used *P. aeruginosa* genomic DNA (eDNA

in *P. aeruginosa* biofilm is derived from random chromosomal DNA) from an exopolysaccharide-non-producing strain (*algC* mutant) (Ma *et al.*, 2012), which eliminated potential interference from exopolysaccharides associated with purified DNA. The results showed that *P. aeruginosa* genomic DNA inhibited the detection of Psl by the anti-Psl antibody (Fig. 5A). *P. aeruginosa* DNA 120  $\mu\text{g } \mu\text{l}^{-1}$  (black column in Fig. 5A) reduced detection of Psl by 50% (compared with the white column in Fig. 5A). When a lower concentration of DNA was used, the inhibition was reduced (grey column in Fig. 5A). These results indicated that DNA can bind to Psl coated on ELISA wells and can thereby interfere with the binding of anti-Psl antibody to Psl, suggesting that Psl physically interacts with *P. aeruginosa* DNA.

To examine whether the interaction between Psl and DNA is specific, we used salmon sperm DNA for the competitive-binding assay. Like *P. aeruginosa* DNA, salmon sperm DNA interfered with the binding of anti-Psl antibody to Psl, and the degree of interference promoted with an increase of salmon sperm DNA concentration (Fig. 5A). This result suggested that Psl polysaccharide can bind to both prokaryotic and eukaryotic DNA.

*P. aeruginosa* and the Gram-positive bacterium *S. aureus* are two prevalent species that often infect CF patients (Harrison, 2007). *P. aeruginosa* can lyse *S. aureus* and other Gram-positive bacteria (Mashburn *et al.*, 2005; Harrison, 2007). Although bacterial DNA can activate neutrophils (Fuxman Bass *et al.*, 2010), the presence of human neutrophils promotes biofilm formation by *P. aeruginosa* (Walker *et al.*, 2005). In addition, human neutrophils can release granule proteins and chromatin that together form extracellular fibres to trap bacteria (Brinkmann *et al.*, 2004), yet most of the trapped bacteria on neutrophils extracellular traps (NETs) remain alive (Menegazzi *et al.*, 2012). *P. aeruginosa* was recently showed to induce NET formation (Yoo *et al.*, 2014). Since the Psl–eDNA interaction is not specific, we tested the hypothesis that *P. aeruginosa* Psl is able to bind the genomic DNA from human neutrophils and *S. aureus* by the competitive binding assay. The results showed that both *S. aureus* and neutrophils DNA inhibited the ability of anti-Psl serum to detect Psl in the ELISA assay, suggesting that Psl can interact with DNA from *S. aureus* and human neutrophils (Fig. 5A). This result also implies that the eDNA–Psl interaction might increase the survival of *P. aeruginosa* in the lungs of CF patients by allowing the bacterial cells of *P. aeruginosa* to use NETs or eDNA from other microbial species as a scaffold on which to grow its own communities. In consistent with our perspective, recent reports also suggested the non-mucoid *P. aeruginosa* strains (produce Psl, but little alginate exopolysaccharide) induces NET formation better than the mucoid strains (produce predominant alginate, but little Psl), and in the case of CF, NET release may actually support initial bacterial sequestration and drive mutability (Dwyer *et al.*, 2014; Rahman and Gadjeva, 2014).

### Modelling of Psl–DNA interaction

To know how Psl may interact with DNA, we used the Glycam Biomolecule Builder to generate an energy-minimized spatial structure model of the Psl repeat unit (Appendix S1). AutoDock software was used to mimic the physical interaction between a single repeat unit of Psl and the DNA double helix. The results suggested that Psl was able to fit into the minor groove of the DNA double helix, allowing hydrogen bonds to form between DNA and Psl

(Fig. 5B). The estimated interaction energy for the Psl–DNA complex was  $-2.18 \text{ kcal mol}^{-1}$ .

### Psl–DNA interaction determined by isothermal titration calorimetry (ITC)

Isothermal titration calorimetry is an important technique to study the thermodynamics of molecular interactions. This technique was recently used to study the binding of protein to lipid polysaccharide (LPS) (Gries *et al.*, 2014). We used ITC to further confirm the interaction between Psl and DNA. Salmon sperm DNA was used to titrate Psl dispersion. Data showed in Fig. 6 indicate an exclusively exothermic reaction, which however does not show a sigmoidal saturation profile. A similar profile was reported for the LPS–protein interaction. The observed enthalpy change of DNA–Psl interaction is in the range of  $-8$  to  $-4.5 \text{ kJ mol}^{-1}$  (Fig. 6A, lower panel), which indicates a binding of salmon sperm DNA to Psl. A variety of Psl/DNA ratios gave similar results (data not shown). When genomic DNA of *P. aeruginosa* was used to titrate Psl, it showed a stronger DNA–Psl interaction with the enthalpy change in range of  $-23$  to  $-6.0 \text{ kJ mol}^{-1}$  (Fig. 6B, lower panel). These results were consistent with the data shown in Fig. 5A, in which *P. aeruginosa* gave better inhibition than salmon sperm DNA.

### Significance of the eDNA–Psl interaction

The Psl–eDNA interaction may benefit biofilms in many ways. First, the interaction allows Psl to associate with eDNA or fusion of multiple DNA strands together to form a super DNA–Psl fibre, which functions as a skeleton of biofilm or gives a backbone support, allowing bacteria to attach with and grow. Second, as a signal molecular, Psl can stimulate bacteria adhered on matrix to synthesize cyclic-di-GMP (Irie *et al.*, 2012), which enhances the production of exopolysaccharide and retains the bacteria in the biofilm communities. Third, the association of eDNA with Psl polysaccharide may limit access of agents that target only one component of biofilm matrix. This was supported by our data that the biofilm of a Psl-deficient strain was more sensitive than its isogenic wild-type strain to DNase I treatment (Fig. S2), and by the previously published finding that DNase I cannot disrupt established, ‘aged’ biofilms (Whitchurch *et al.*, 2002). Fourth, a high concentration of eDNA was suggested to cause chelating cations to lyse bacterial cells (Mulcahy *et al.*, 2008), and the covering of eDNA by Psl might reduce this cationchelating of eDNA in biofilm and protect bacteria. Finally, the eDNA–Psl interaction might increase *P. aeruginosa* survival in multispecies biofilms or within a human host because Psl of *P. aeruginosa* could interact with DNA from other bacteria as well as DNA from human neutrophils, which might enable *P. aeruginosa* to attach on NET or eDNA from other bacteria to grow its biofilms.

*Pseudomonas aeruginosa* can also produce an exopolysaccharide named Pel, which is required for pellicles formation. Reports have shown that *P. aeruginosa* strain, such as PAO1, primarily uses Psl as matrix component (Ma *et al.*, 2009; Colvin *et al.*, 2012). We have previously demonstrated that the formation of Psl fibres does not require Pel. The purified Psl used in this study was prepared from PAO1-derived strain WFP801 (Psl-overproduced strain), which has reported to produce little Pel (Wang *et al.*, 2013).

Therefore, it is unlikely that Pel could be involved in the eDNA–Psl association or interaction in pellicles.

## Conclusion

Our data suggest that the two main biofilm matrix components of *P. aeruginosa*, eDNA and Psl, cooperate by physically interacting in a biofilm to form the web of Psl–eDNA fibres, which functions as a skeleton to allow bacteria to adhere and grow. Bacterial membrane is overlapped with eDNA or Psl fibres, suggesting the plausible formation of eDNA–Psl–membrane fibres in biofilms. Once the eDNA–Psl–membrane combined matrix forms, the biofilm and matrix are protected against DNase I, or agents targeted one kind of biofilm matrix components. Psl can interact with DNA from diverse sources, suggesting that *P. aeruginosa* has the ability to use DNA of other organisms (such as human neutrophils and other bacterial species) as a scaffold to form its own communities. DNA was reported to interact with glucan (Sakurai and Shinkai, 2001). In this study, we showed that DNA interacted with Psl, a repeating pentasaccharide containing D-mannose, D-glucose and L-rhamnose. This suggests that DNA may interact with different kinds of polysaccharide, and the strategy used in *P. aeruginosa* biofilm formation might be common for bacteria in natural and clinical settings. Taken together, the formation of biofilm matrix is a complex, dynamic process with contribution of multiple factors, including bacterial migration, cell death, the release of polysaccharide and eDNA, and the interaction between the matrix components.

## Experimental procedures

### Strains and growth conditions

The *P. aeruginosa* strains used in this study are listed in Table S1. Unless otherwise indicated, *P. aeruginosa* was grown at 37°C in Luria–Bertani medium lacking sodium chloride (LBNS) or in Jensen's, a chemically defined medium (Ma *et al.*, 2006). Biofilms of *P. aeruginosa* were cultured in Jensen's medium at room temperature (RT). To induce the transcription of the *psl* operon, 0.2–2.0% arabinose was added to Jensen's medium.

### Biofilm and matrix staining

The air–liquid interface biofilms were grown in glass chambers with individual chamber dimensions of 1 × 1 × 4 cm (Chambered #1.5 German Coverglass System, Nunc) as described previously (Wang *et al.*, 2013). DNase I (Sigma, 100 U/chamber) was added to glass chambers 1 h post-inoculation. For Confocal Laser Scanning Microscopy (CLSM) observation, buffer was gently removed from glass chambers to allow the pellicles to drop onto coverslips. The flow-cell biofilms were grown at RT in three-channel flow cell with individual channel dimensions of 1 × 4 × 40 mm (Stovall Life Science) as previously described (Ma *et al.*, 2006). The mid-log phase culture was used for inoculation. The biofilms were stained with membrane stain FM4-64 (1 µm ml<sup>-1</sup> final concentration, Molecular Probes, Invitrogen) or DNA stain SYTO9 (Molecular Probes, Invitrogen). Extracellular DNA in biofilms was stained with PI and SYTOX Green (Molecular Probes,

Invitrogen). The Psl matrix was stained with fluorescence-labelled lectin HHA at  $100 \mu\text{g ml}^{-1}$  (EY Lab) as we described elsewhere (Ma *et al.*, 2009).

### Image acquisition and analysis

All fluorescent images were acquired with a Zeiss 510 CLS microscope (Carl Zeiss, Jena, Germany). Images were obtained using a  $63\times/1.3$  objective. An LSM image browser generated the 3D images and optical Z-sections. CLSM-captured images were subjected to quantitative image analysis using COMSTAT software to determine biofilm biomass, thickness and other properties as previously described (Heydorn *et al.*, 2000). The biofilm biomass was quantified from SYTO9-stained images or by crystal violet staining of pellicles. ImageJ software was used to analyse the colocalization of eDNA and Psl and to make the corresponding colour map (Hartig, 2013; Zinchuk *et al.*, 2011). The colocalization coefficient and correlation coefficient of eDNA and Psl in biofilm images were analysed and calculated as previously described (Zinchuk *et al.*, 2013).

### DNA purification

Salmon sperm DNA was obtained from Sigma-Aldrich. Neutrophils were isolated from the whole blood of healthy volunteers (25–35 years old) by dextral sedimentation, followed by Ficoll-Hypaque density-gradient centrifugation (400 g, 30 min) as described previously. Erythrocytes were removed by hypotonic lysis (Ottoneo *et al.*, 1999). Genomic DNAs of neutrophils, *P. aeruginosa* and *S. aureus* ATCC 6538 were purified with Wizard Genomic DNA Purification Kits (Promega).

### Preparation of Psl extract

Psl polysaccharide extract was prepared from overnight culture of WFPA801 as previously described (Byrd *et al.*, 2009) with modification. To remove the DNA, crude Psl polysaccharide was precipitated with three volumes of ethanol and dissolved in pyrogen-free distilled water with 5 mM  $\text{MgCl}_2$ , followed by DNase I (Sigma) treatment ( $0.1 \text{ mg ml}^{-1}$  final concentration) for 5 h at  $37^\circ\text{C}$  and treatment with proteinase K ( $0.1 \text{ mg ml}^{-1}$  final concentration) for 1 h at  $60^\circ\text{C}$ . Psl samples without DNase I treatment were only treated with proteinase K. Enzymes were inactivated at  $80^\circ\text{C}$  for 30 min, and Psl samples were quantified by ELISA as described previously (Byrd *et al.*, 2009).

### Examination of the Psl–DNA interaction by ELISA

To determine Psl and DNA interact, Psl post-treatment of DNase and proteinase was diluted with phosphate buffer (PBS, 0.01 M phosphate, 0.15 M NaCl; pH 7.2), and Psl at  $0.25 \mu\text{g ml}^{-1}$  was used to coat 96-well MaxiSorp plates (Jet Biofil,  $100 \mu\text{l/well}$ ) for overnight at  $4^\circ\text{C}$ . Psl-coated plates were washed five times with PBST buffer (PBS containing 0.05% Tween 20) and were blocked for 2 h at RT with 10% newborn calf serum (MP chromato Pur) in PBS. DNA from different origins was diluted in PBS to 60, 90 or  $120 \mu\text{g ml}^{-1}$ . An aliquot of DNA ( $100 \mu\text{l}$  per well) was transferred into the Psl-coated plates and incubated overnight at  $4^\circ\text{C}$ . After five washes with PBST, Psl was detected with anti-Psl serum as previously described. The absorbance at 450 nm (A450) was determined by the Multiskan Ascent version 2.6 plate reader.



### Isothermal titration calorimetry

Microcalorimetric measurements of the binding of salmon sperm DNA to Psl were performed on a NANO ITC 2G at 25°C (TA Instruments, USA) as described previously with modification (Ni *et al.*, 2013). Psl and salmon sperm DNA were dissolved into 0.01 M PBS (pH 7.4). Psl (2.25 mg ml<sup>-1</sup>) was dispensed into the microcalorimetric cell (volume 1.3 ml), and the DNA solution (200 µg ml<sup>-1</sup>) was filled into the syringe compartment (volume 250 µl). DNA was titrated in 10 µl portions (3.14 µl for the first injection) into the Psl-containing cell under constant stirring, and the heat of reaction was plotted versus time. Data analysis was executed by the N<sub>ANO</sub>ANALYZE software.

### Modelling of the DNA–Psl interaction by docking

The spatial structure of the DNA duplex in an ideal B-DNA conformation for docking was obtained by using the w<sub>3</sub>DNA software package (Zheng *et al.*, 2009). Docking calculations were carried out using A<sub>UTO</sub>D<sub>OCK</sub> version 4.2 with general protocols (Morris *et al.*, 2008). The averaged conformations of the Psl polysaccharide repeat unit (generated from molecular dynamics (MD) simulation, see Appendix S1) and the DNA duplex were converted into the proper file formats for A<sub>UTO</sub>D<sub>OCK</sub> using A<sub>UTO</sub>D<sub>OCK</sub> Tools version 1.5.4 (Morris *et al.*, 2009). The DNA was enclosed in a box with 70 × 70 × 70 grid points in x × y × z directions and a grid spacing of 0.375 Å. The maximum number of energy evaluation was set to 2.5 × 10<sup>6</sup>, and the number of Lamarckian genetic algorithm runs was set to 100. Lamarckian genetic algorithms, as implemented in A<sub>UTO</sub>D<sub>OCK</sub>, were used to perform docking calculations. During the docking, Psl was kept in a flexible state while the DNA was kept in fixed state. All other parameters were given default settings. One hundred solutions were generated for the docking run. The docking results were then subjected to cluster analysis (RMS tolerance of 2.0 Å), and the lowest energy conformation was selected. The docked structure suggested that the Psl polysaccharide repeat unit fitted the minor groove of DNA and was almost parallel with the DNA helix. The estimated interaction energy for the polysaccharide-DNA complex was -2.18 kcal mol<sup>-1</sup>. The complex was stabilized by hydrogen bonds.

### Supplementary Material

Refer to Web version on PubMed Central for supplementary material.

### Acknowledgments

The authors thank Dr. Alan K Chang at Liaoning University, Dr. Joseph Lam at the University of Guelph, and Dr. Di Wang and Dr. Qing Wei at the Institute of Microbiology, Chinese Academy of Sciences, for their contribution to the revision of the manuscript; Dr. Tong Li at Peking University for assistance with isolation of neutrophils; Mr. Likai Hao at Eberhard Karls University Tuebingen for assistance with image analysis. This work was supported by the National Basic Research Program of China (973 Program, Grant 2014CB846002) (L.Z.M.) and the National Natural Science Foundation of China Grant 31270177 (L.Z.M.).

### References

Allesen-Holm M, Barken KB, Yang L, Klausen M, Webb JS, Kjelleberg S, et al. A characterization of DNA release in *Pseudomonas aeruginosa* cultures and biofilms. *Mol Microbiol.* 2006; 59:1114–1128. [PubMed: 16430688]

- Brinkmann V, Reichard U, Goosmann C, Fauler B, Uhlemann Y, Weiss DS, et al. Neutrophil extracellular traps kill bacteria. *Science*. 2004; 303:1532–1535. [PubMed: 15001782]
- Byrd MS, Sadovskaya I, Vinogradov E, Lu HP, Sprinkle AB, Richardson SH, et al. Genetic and biochemical analyses of the *Pseudomonas aeruginosa* Psl exopolysaccharide reveal overlapping roles for polysaccharide synthesis enzymes in Psl and LPS production. *Mol Microbiol*. 2009; 73:622–638. [PubMed: 19659934]
- Byrd MS, Pang B, Mishra M, Swords WE, Wozniak DJ. The *Pseudomonas aeruginosa* exopolysaccharide Psl facilitates surface adherence and NF-kappaB activation in A549 cells. *MBio*. 2010; 1:e00140–10. [PubMed: 20802825]
- Chiang WC, Nilsson M, Jensen PO, Hoiby N, Nielsen TE, Givskov M, Tolker-Nielsen T. Extracellular DNA shields against aminoglycosides in *Pseudomonas aeruginosa* biofilms. *Antimicrob Agents Chemother*. 2013; 57:2352–2361. [PubMed: 23478967]
- Colvin KM, Irie Y, Tart CS, Urbano R, Whitney JC, Ryder C, et al. The Pel and Psl polysaccharides provide *Pseudomonas aeruginosa* structural redundancy within the biofilm matrix. *Environ Microbiol*. 2012; 14:1913–1928. [PubMed: 22176658]
- Costerton JW, Stewart PS, Greenberg EP. Bacterial biofilms: a common cause of persistent infections. *Science*. 1999; 284:1318–1322. [PubMed: 10334980]
- Dominiak DM, Nielsen JL, Nielsen PH. Extracellular DNA is abundant and important for microcolony strength in mixed microbial biofilms. *Environ Microbiol*. 2011; 13:710–721. [PubMed: 21118344]
- Dwyer M, Shan Q, D'Ortona S, Maurer R, Mitchell R, Olesen H, et al. Cystic fibrosis sputum DNA has NETosis characteristics and neutrophil extracellular trap release is regulated by macrophage migration-inhibitory factor. *J Innate Immun*. 2014; 6:765–779. [PubMed: 24862346]
- Flemming HC, Wingender J. The biofilm matrix. *Nat Rev Microbiol*. 2010; 8:623–633. [PubMed: 20676145]
- Fuxman Bass JI, Russo DM, Gabelloni ML, Geffner JR, Giordano M, Catalano M, et al. Extracellular DNA: a major proinflammatory component of *Pseudomonas aeruginosa* biofilms. *J Immunol*. 2010; 184:6386–6395. [PubMed: 20421641]
- Gloag ES, Turnbull L, Huang A, Vallotton P, Wang H, Nolan LM, et al. Self-organization of bacterial biofilms is facilitated by extracellular DNA. *Proc Natl Acad Sci USA*. 2013; 110:11541–11546. [PubMed: 23798445]
- Gries A, Prassl R, Fukuoka S, Rossle M, Kaconis Y, Heinbockel L, et al. Biophysical analysis of the interaction of the serum protein human beta2GPI with bacterial lipopolysaccharide. *FEBS Open Bio*. 2014; 4:432–440.
- Harrison F. Microbial ecology of the cystic fibrosis lung. *Microbiology*. 2007; 153:917–923. [PubMed: 17379702]
- Hartig SM. Basic image analysis and manipulation in ImageJ. *Curr Protoc Mol Biol*. 2013; 102:14.15.1–14.15.12.
- Heydorn A, Nielsen AT, Hentzer M, Sternberg C, Givskov M, Ersboll BK, Molin S. Quantification of biofilm structures by the novel computer program COMSTAT. *Microbiology*. 2000; 146:2395–2407. [PubMed: 11021916]
- Irie Y, Borlee BR, O'Connor JR, Hill PJ, Harwood CS, Wozniak DJ, Parsek MR. Self-produced exopolysaccharide is a signal that stimulates biofilm formation in *Pseudomonas aeruginosa*. *Proc Natl Acad Sci USA*. 2012; 109:20632–20636. [PubMed: 23175784]
- Kolodkin-Gal I, Cao S, Chai L, Bottcher T, Kolter R, Clardy J, Losick R. A self-produced trigger for biofilm disassembly that targets exopolysaccharide. *Cell*. 2012; 149:684–692. [PubMed: 22541437]
- Ma L, Jackson KD, Landry RM, Parsek MR, Wozniak DJ. Analysis of *Pseudomonas aeruginosa* conditional *psl* variants reveals roles for the *psl* polysaccharide in adhesion and maintaining biofilm structure postattachment. *J Bacteriol*. 2006; 188:8213–8221. [PubMed: 16980452]
- Ma L, Conover M, Lu H, Parsek MR, Bayles K, Wozniak DJ. Assembly and development of the *Pseudomonas aeruginosa* biofilm matrix. *PLoS Pathog*. 2009; 5:e1000354. [PubMed: 19325879]
- Ma L, Wang J, Wang S, Anderson EM, Lam JS, Parsek MR, Wozniak DJ. Synthesis of multiple *Pseudomonas aeruginosa* biofilm matrix exopolysaccharides is post-transcriptionally regulated. *Environ Microbiol*. 2012; 14:1995–2005. [PubMed: 22513190]

- Mashburn LM, Jett AM, Akins DR, Whiteley M. *Staphylococcus aureus* serves as an iron source for *Pseudomonas aeruginosa* during in vivo coculture. *J Bacteriol.* 2005; 187:554–566. [PubMed: 15629927]
- Menegazzi R, Declava E, Dri P. Killing by neutrophil extracellular traps: fact or folklore? *Blood.* 2012; 119:1214–1216. [PubMed: 22210873]
- Molin S, Tolker-Nielsen T. Gene transfer occurs with enhanced efficiency in biofilms and induces enhanced stabilisation of the biofilm structure. *Curr Opin Biotechnol.* 2003; 14:255–261. [PubMed: 12849777]
- Morris GM, Huey R, Olson AJ. Using AutoDock for ligand-receptor docking. *Curr Protoc Bioinformatics.* 2008; 8:8.14.1–8.14.40.
- Morris GM, Huey R, Lindstrom W, Sanner MF, Belew RK, Goodsell DS, Olson AJ. AutoDock4 and AutoDockTools4: automated docking with selective receptor flexibility. *J Comput Chem.* 2009; 30:2785–2791. [PubMed: 19399780]
- Mulcahy H, Charron-Mazenod L, Lewenza S. Extracellular DNA chelates cations and induces antibiotic resistance in *Pseudomonas aeruginosa* biofilms. *PLoS Pathog.* 2008; 4:e1000213. [PubMed: 19023416]
- Ni B, Huang Z, Fan Z, Jiang CY, Liu SJ. *Comamonas testosteroni* uses a chemoreceptor for tricarboxylic acid cycle intermediates to trigger chemotactic responses towards aromatic compounds. *Mol Microbiol.* 2013; 90:813–823. [PubMed: 24102855]
- Ottone L, Tortolina G, Amelotti M, Dallegri F. Soluble Fas ligand is chemotactic for human neutrophilic polymorphonuclear leukocytes. *J Immunol.* 1999; 162:3601–3606. [PubMed: 10092820]
- Parks QM, Young RL, Poch KR, Malcolm KC, Vasil ML, Nick JA. Neutrophil enhancement of *Pseudomonas aeruginosa* biofilm development: human F-actin and DNAs targets for therapy. *J Med Microbiol.* 2009; 58:492–502. [PubMed: 19273646]
- Rahman S, Gadjeva M. Does NETosis contribute to the bacterial pathoadaptation in cystic fibrosis? *Front Immunol.* 2014; 5:378.10.3389/fimmu.2014.00378 [PubMed: 25157250]
- Sakurai K, Shinkai S. Novel DNA-polysaccharide triple helices and their application to a gene carrier. *J Incl Phenom Macrocycl Chem.* 2001; 41:173–178.
- Singh PK, Schaefer AL, Parsek MR, Moninger TO, Welsh MJ, Greenberg EP. Quorum-sensing signals indicate that cystic fibrosis lungs are infected with bacterial biofilms. *Nature.* 2000; 407:762–764. [PubMed: 11048725]
- Walker TS, Tomlin KL, Worthen GS, Poch KR, Lieber JG, Saavedra MT, et al. Enhanced *Pseudomonas aeruginosa* biofilm development mediated by human neutrophils. *Infect Immun.* 2005; 73:3693–3701. [PubMed: 15908399]
- Wang S, Parsek MR, Wozniak DJ, Ma LZ. A spider web strategy of type IV pili-mediated migration to build a fibre-like Psl polysaccharide matrix in *Pseudomonas aeruginosa* biofilms. *Environ Microbiol.* 2013; 15:2238–2253. [PubMed: 23425591]
- Whitchurch CB, Tolker-Nielsen T, Ragas PC, Mattick JS. Extracellular DNA required for bacterial biofilm formation. *Science.* 2002; 295:1487. [PubMed: 11859186]
- Xiao J, Klein MI, Falsetta ML, Lu B, Delahunty CM, Yates JR, et al. The exopolysaccharide matrix modulates the interaction between 3D architecture and virulence of a mixed-species oral biofilm. *PLoS Pathog.* 2012; 8:e1002623. [PubMed: 22496649]
- Yoo DG, Floyd M, Winn M, Moskowitz SM, Rada B. NET formation induced by *Pseudomonas aeruginosa* cystic fibrosis isolates measured as release of myeloperoxidase-DNA and neutrophil elastase-DNA complexes. *Immunol Lett.* 2014; 160:186–194. [PubMed: 24670966]
- Zhao K, Tseng BS, Beckerman B, Jin F, Gibiansky ML, Harrison JJ, et al. Psl trails guide exploration and microcolony formation in *Pseudomonas aeruginosa* biofilms. *Nature.* 2013; 497:388–391. [PubMed: 23657259]
- Zheng G, Lu XJ, Olson WK. Web 3DNA – a web server for the analysis, reconstruction, and visualization of three-dimensional nucleic-acid structures. *Nucleic Acids Res.* 2009; 37:W240–W246. [PubMed: 19474339]

Zinchuk V, Wu Y, Grossenbacher-Zinchuk O, Stefani E. Quantifying spatial correlations of fluorescent markers using enhanced background reduction with protein proximity index and correlation coefficient estimations. *Nat Protoc.* 2011; 6:1554–1567. [PubMed: 21959238]

Zinchuk V, Wu Y, Grossenbacher-Zinchuk O. Bridging the gap between qualitative and quantitative colocalization results in fluorescence microscopy studies. *Sci Rep.* 2013; 3:1365.10.1038/srep01365 [PubMed: 23455567]

Author Manuscript

Author Manuscript

Author Manuscript

Author Manuscript

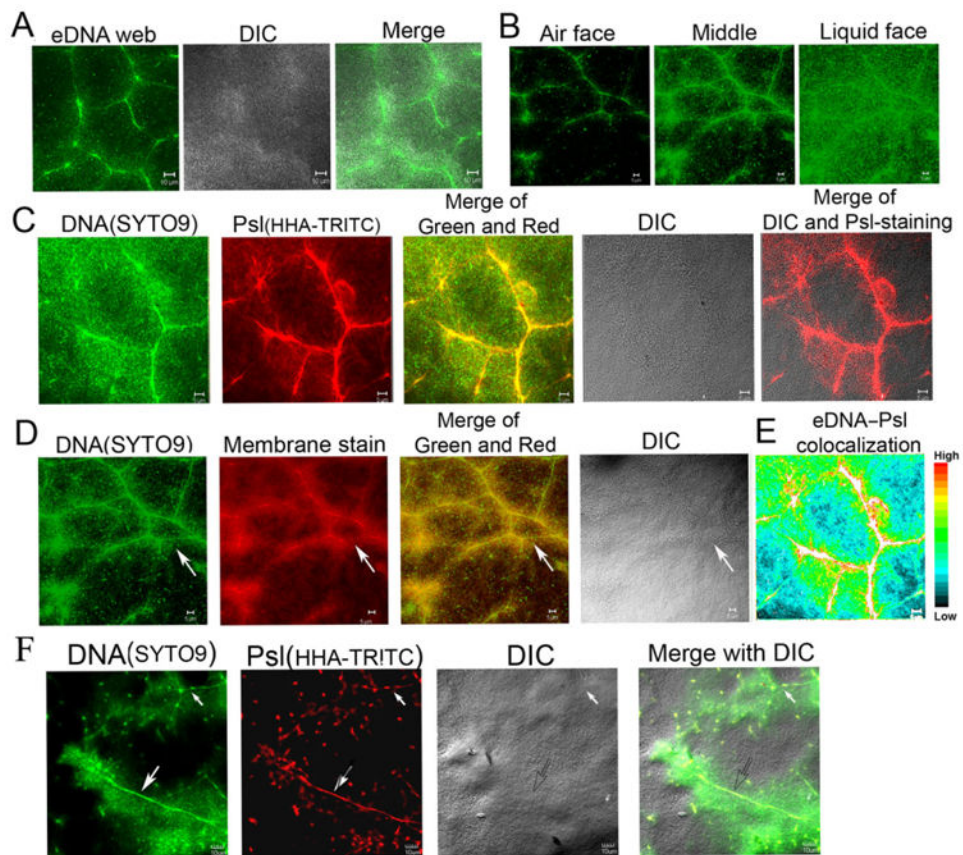


**Fig. 1.**

The web of DNA fibres and its association with Psl polysaccharide and bacterial cell membrane in the air–liquid interface biofilms (pellicles) of *P. aeruginosa*.

A. A web of fibre-like DNA (stained in green by SYTO9) was clearly visualized at the middle of pellicles grown at air–liquid interface of standing culture.

B. The optical sectioned images showed the location of eDNA fibres web (green) in a pellicle.

C. The eDNA fibres web (green) was associated with the fibres of Psl polysaccharide (stained in red by lectin HHA-TRITC) in pellicles.

D. The eDNA fibres were colocalized with bacterial membrane in a 46 h pellicle stained by SYTO9 and the cell membrane stained by FM6-64 (the arrow indicated the eDNA-membrane fibres web).

E. The eDNA–Psl colocalization was mostly associated with the fibre-like matrix structure depicted by the colour map, which was made by the *IMAGEJ* software according to the colour image series of (C).

F. The eDNA–Psl fibres with strong (indicated by a big arrow) or weak (indicated by a small arrow) fluorescent signal both found in the middle of a pellicle. Scale bar in all panels: 5  $\mu\text{m}$ .

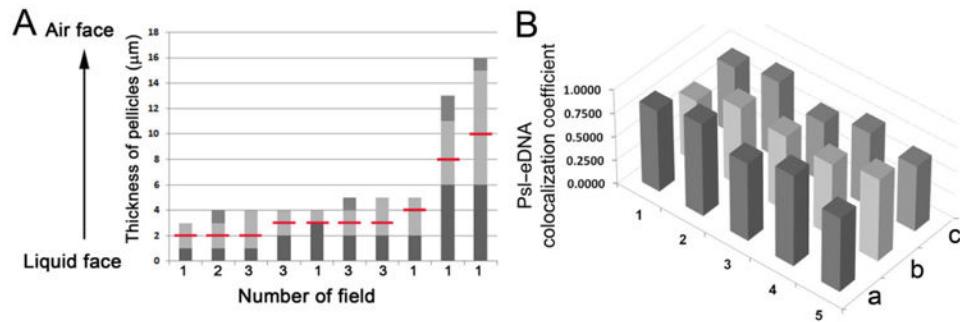


**Fig. 2.**

The area in pellicles found eDNA–Psl fibres and the analysis of eDNA–Psl colocalization coefficients.

A. Analysis of 19 CLSM image stacks from 2-day old pellicles showed the thickness of pellicles, the area (light grey columns) with eDNA–Psl fibres, and the location found the eDNA–Psl fibres with highest fluorescent intensity (indicated by the red lines).

B. Columns showed the eDNA–Psl colocalization coefficients analysed from five images (No #1–5) by three methods. a, Pearson's correlation coefficient; b, Manders' colocalization coefficient M1; c, Manders' colocalization coefficient M2.

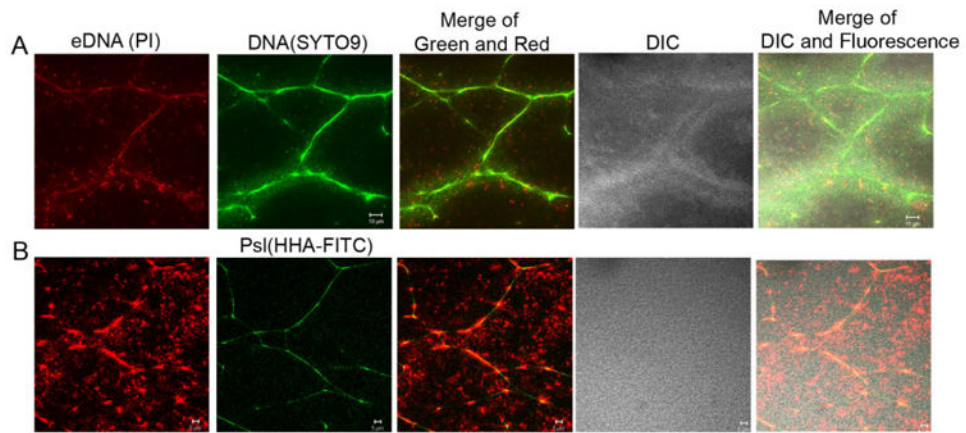


**Fig. 3.** The eDNA and dead bacteria in pellicles of *P. aeruginosa* PAO1 were stained by Propidium iodide (PI) to confirm that fibre-like DNA was eDNA. Shown were the optical sectioned images in the middle of pellicles. (A) PI (red) and SYTO9 (green) double-stained images of a 2-day-old pellicle. (B) PI (red) and HHA-FITC (a lectin that stains Psl in green) double-stained images of a 2-day-old pellicle. Scale bar: 10  $\mu\text{m}$  for (A); 5  $\mu\text{m}$  for (B).

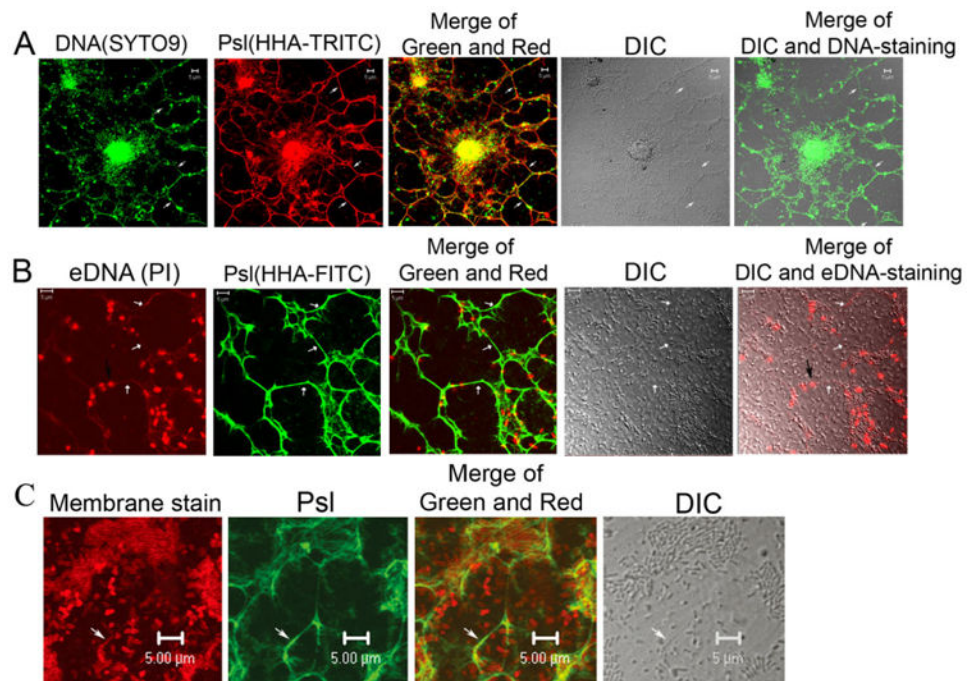


**Fig. 4.**

The eDNA–Psl fibres in flow-cell biofilms of *P. aeruginosa*.

A. SYTO9 and Psl staining (HHA-TRITC) showed the colocalization of Psl fibres with eDNA in a flow-cell biofilm.

B. eDNA fibres (stained in red by PI) were colocalized with Psl fibres (stained in green by lectin HHA-FITC) in a flow-cell biofilm. The black arrow indicated the dead bacteria associated with the eDNA–Psl fibres. The white arrows indicated the visible eDNA–Psl fibres on DIC images.

C. A track of bacterial membrane (stain in red by FM4-64) was colocalized with Psl (green, stained by HHA-FITC) in a flow-cell biofilm. The white arrow indicated a Psl-membrane track and its corresponding DIC image. Scale bar in all panels: 5 µm.



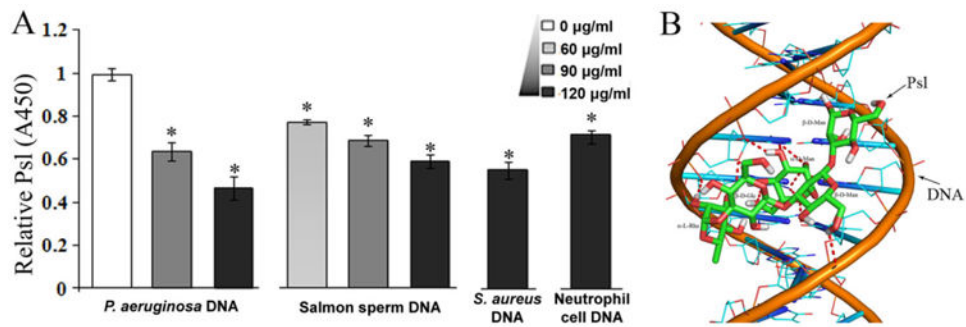


**Fig. 5.**

The interaction between DNA and Psl polysaccharide.

A. The detection of Psl can be interfered by DNA isolated from *P. aeruginosa*, salmon sperm, *S. aureus* and neutrophil cells. Psl was detected by anti-Psl antibody in ELISA assay. The samples without DNA blocking were normalized to 1 ( $A_{450} = 0.635 \pm 0.012$ ).  $*P < 0.01$ .

B. A plausible model for DNA–Psl interaction. The docking result suggested that hydrogen bonds (indicated by dash lines) can be formed between a Psl polysaccharide repeat unit (carbon, green; oxygen, red; hydrogen, white) and the standard B-DNA duplex (phosphorus, orange; carbon, cyan; oxygen, red; nitrogen, blue).

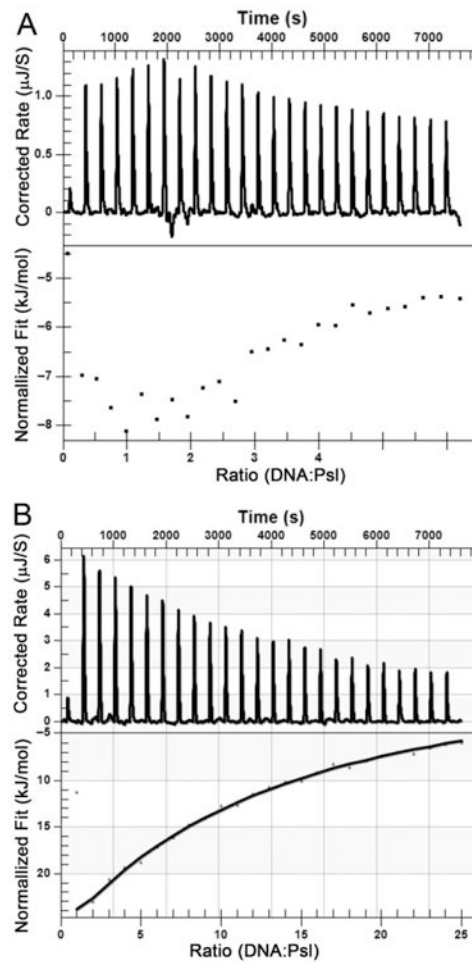


**Fig. 6.** Isothermal titration calorimetry measurement to determine the interaction of Psl and salmon sperm DNA.  
 A. Salmon sperm DNA to titrate Psl dispersion.  
 B. The genomic DNA of *P. aeruginosa* to titrate Psl dispersion. The upper panel shows raw titration data, and the bottom panel is integrated and dilution-corrected peak area plotting of titration data. To a Psl dispersion ( $2.25 \text{ mg ml}^{-1}$ ), DNA ( $200 \text{ } \mu\text{g ml}^{-1}$ ) is titrated in  $10 \text{ } \mu\text{l}$  portion.